Simulation of Post-Frontal Boundary Layers Observed During the ARM 2000 Cloud IOP

D. B. Mechem and Y. L. Kogan
Cooperative Institute for Mesoscale Meteorological Studies
University of Oklahoma
Norman, Oklahoma

M. Poellot
University of North Dakota
Grand Forks, North Dakota

Introduction

Large-eddy simulation (LES) models have been widely employed in the study of radiatively forced cloud topped boundary layers (CTBL). These boundary layers are typically well mixed and characterized by a sharp jump in temperature and moisture, marking the transition between boundary layer and free troposphere (e.g., Moeng 1986). Shallow cumulus, forced by strong surface fluxes, have also been investigated (e.g., Krueger and Bergeron 1994; Brown et al. 2001), as have stable boundary layers in which the static energy increases with height (e.g., Kosovic and Curry 2000). One advantage of investigating well mixed boundary layers is that they are amenable to theoretical constructs (e.g., mixed layer scalings), which to date have not been as thoroughly developed for more general boundary layer conditions. It appears that these more general planetary boundary layers (PBLs) are less understood.

Two cases of general boundary layer cloud were observed during the Atmospheric Radiation Measurement (ARM) Program March 2000 cloud intensive operational period (IOP). This IOP was centered at the ARM Southern Great Plains (SGP) Cloud and Radiation Testbed (CART) in Northern Oklahoma. These two cases are not typical well-mixed CTBLs and are unique in several ways. Both occur after the passage of cold fronts and contain cloud regions colder than 0°C. The first case occurs in an environment of large-scale subsidence divergence, while the second case is characterized by significant upward vertical motion associated with a nearby cold front. The first case is well mixed, but the sharp inversion structure found in most CTBLs is not present, nor is a sharp distinction in cloud top liquid water. The cloud in the second case is over 3 km deep, with a complex vertical thermodynamic distribution. The structure includes a well-mixed surface layer, a deep layer characterized by significant thermal stratification, and a less stable, radiatively driven layer at cloud top.

In this study, we summarize our preliminary attempts at using the technique of LES to investigate these two cases of general boundary layer cloud observed during the IOP. The University of North Dakota Citation flew on both days, collecting in situ state and microphysical data. The LES is initialized with thermodynamic data from aircraft and aerosol spectra inferred from aircraft microphysical measurements, which can subsequently be used to critique LES performance. We will show that the

LES produces clouds that are reasonable compared to the aircraft observations. Preliminary analysis also indicates agreement with previous, well-mixed CTBL studies on microphysical grounds.

Methodology

We use the Cooperative Institute for Mesoscale Meteorology Studies LES model, as described in Kogan et al. (1995) and Khairoutdinov and Kogan (1999). The LES includes an explicit representation of microphysical processes, solving prognostic equations for 19 categories of cloud condensation nuclei and 25 categories of liquid droplets. This model has been show to perform well, reproducing observed droplet side distributions and boundary layer structure.

The simulations are run for 6 hours with a horizontal grid spacing of 100 m, and vertical grid spacings of 50 m (shallow, March 3 case) and 100 m (deep, March 18 case). For both cases, the model is initialized with profiles of thermodynamic and microphysical data observed from the UND Citation. The model uses virtual liquid water potential temperature (θ_v) and total water (q_t) as prognostic variables, and some measure of cloud liquid water is helpful in obtaining reasonable initial profiles of these.

The overall CCN concentration is inferred by assuming that cloud droplet concentration observed by the forward scattering spectrometer probe (FSSP) instrument is a proxy for activated CCN. CCN spectra shapes are assumed to be lognormal with a mean radius of 0.1 μm and standard deviation of 1.5 μm. Only the total (integrated) concentration differs between the two cases—both cases have the same aerosol spectral shape. Some regions of the cloud in both cases are below 0°C. For the purposes of this study, we assume that the clouds are solely composed of liquid water.

Although both cases are post-frontal, local temperature changes are not particularly large during the time considered, so advective tendencies are neglected. Large-scale forcing is considered, however, in the form of large-scale ascent or descent, as inferred from the 700 mb Eta model omega field. Surface fluxes are taken from the ARM eddy correlation instrument and are set at 30 W m^{-2} for both sensible and latent heat flux. For the calculation of shortwave (SW) radiative transfer, the solar zenith angle is set to 60°.

Shallow, Well-Mixed PBL Case (March 3, 2000)

Figure 1 shows the cloud structure as observed by satellite just before the time of interest. At this time, the surface cold front lay 30 km to the south of the location sampled by aircraft. Winds were largely northerly, and large-scale subsidence dominated.

Aircraft supplied data from which we constructed the profiles of θ_v, q_t, and momentum used to initialize the model (Figure 2). The temperature and total water profiles describe a well-mixed layer 80 m deep, with moderate stratification of the free troposphere above. The aircraft data seemed to show a weak temperature inversion but very little in the way of any moisture jump across the top of the boundary layer. Unlike the CTBL conceptual model, the aircraft observed the presence of cloud up to several

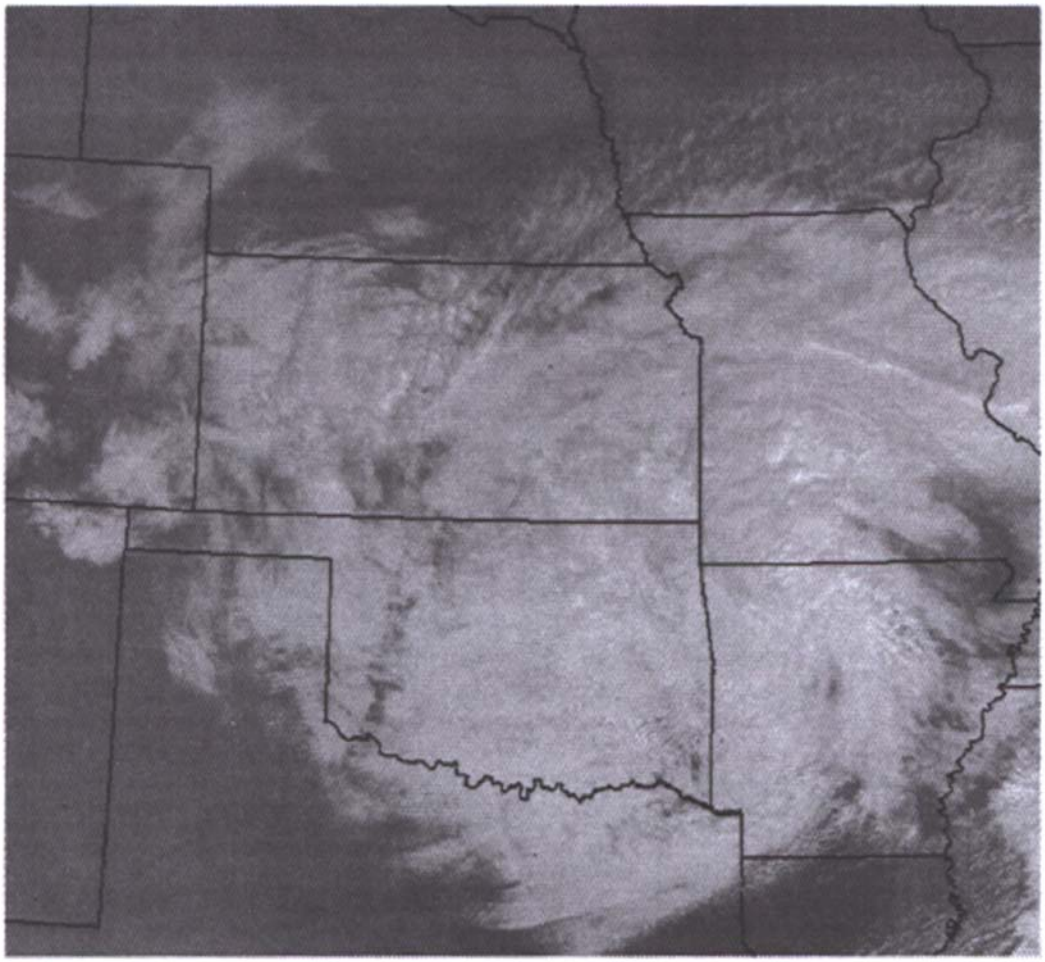

Figure 1. GOES visible imagery from 1632 Universal Time Coordinates (UTC) on March 3, 2002.

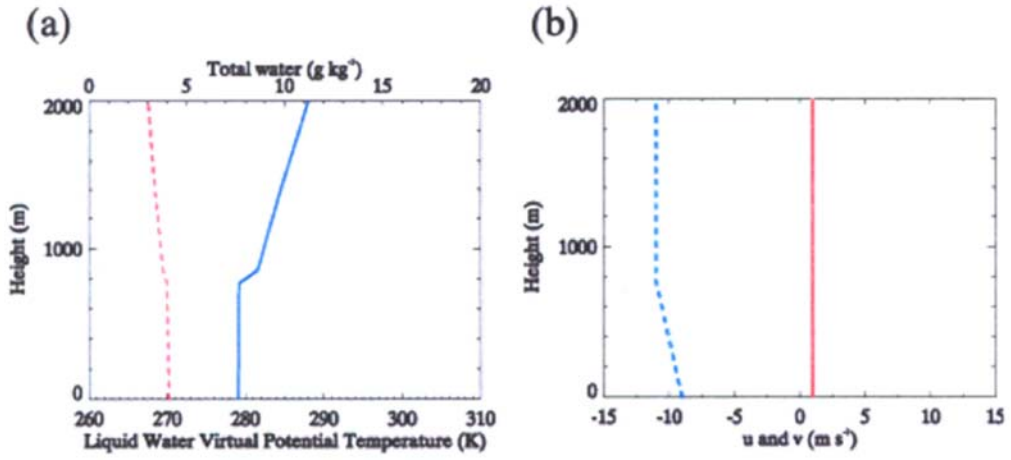

Figure 2. Initial profiles for the March 3, 2000, case. (a) θ_v (solid/blue) and q_t (dashed/red); (b) u (solid/red) and v (dashed/blue).

hundred meters above the weak inversion. Total CCN concentration was taken to be 305 cm^{-3}, a characteristic value for air of continental origin. A weak northerly shear was prescribed throughout the depth of the PBL.

Figure 3 shows a snapshot of the LES behavior for the case after 4 hours of integration. The model required time to "spin up," meaning time to establish reasonable boundary layer structure in the dynamic and microphysical fields, so the model time will not correspond perfectly to the time of the aircraft observations. Even under moderate subsidence, the initial weak temperature inversion dissipates with time (Figure 3a), a result of a 1.5 K warming of the PBL and the free troposphere becoming more stratified under subsidence. The PBL is clearly remaining well mixed, however. Because of the lack of a strong inversion, the liquid water profile (Figure 3b) does not display the sharp vertical gradient at cloud top typical of most CTBLs. In fact, liquid water appears to be present in small quantities as high as 150 m above the weak inversion base.

Profiles of radiative flux (Figure 3c and d) indicate weak SW absorption throughout the depth of the cloud and longwave (LW) flux divergence (cooling) over a layer at the top of the cloud that is deep compared to most CTBLs. The peak of the vertical velocity variance (Figure 3e) is low relative to the depth of the boundary layer, possibly implying that the dominant energy source for the turbulent eddies comes from surface fluxes and stresses rather than cloud top cooling. In this comparatively clean case, little precipitation is produced (Figure 3f), and the cloud remains unbroken throughout the entire simulation (Figure 3g). The CCN concentration shows the main cloud layer in the boundary layer and the presence of a secondary layer above the inversion.

It appears that the weak inversion is the best explanation for why these results differ from those of a typical stratocumulus simulation. The weak vertical temperature and moisture gradients lead to an ambiguity in cloud top and a disorganized distribution in LW forcing. Despite this, the boundary layer remains well mixed.

A comparison of the simulated and observed microphysical character of the March 3 system is shown in Figure 4. The LES is initialized with a large CCN concentration thought to represent polluted, continental air. As such, it produces little precipitation. The observations show a significant tail of larger (drizzle) droplets in the distribution not captured by the model. The model produces a reasonable cloud droplet mode, though it is slightly biased toward smaller droplets. The total (integrated) cloud droplet concentration in the model is compared to that observed by aircraft in Figure 5. Peak concentration in the model agrees well with the FSSP, though the maximum is located slightly lower. The model represents regions of liquid water above the inversion as a secondary maximum, while the observations show a monotonic decrease with height.

Deep, Stable PBL Cloud Case (March 18, 2000)

Figure 6 shows from an Eulerian standpoint the evolution of the cloud system on March 18. Over the course of the day, a boundary layer with patches of intermittent drizzle undergoes a transition, almost a discontinuity, when a cold front passes over the radar. The deep layer of precipitating cloud beginning

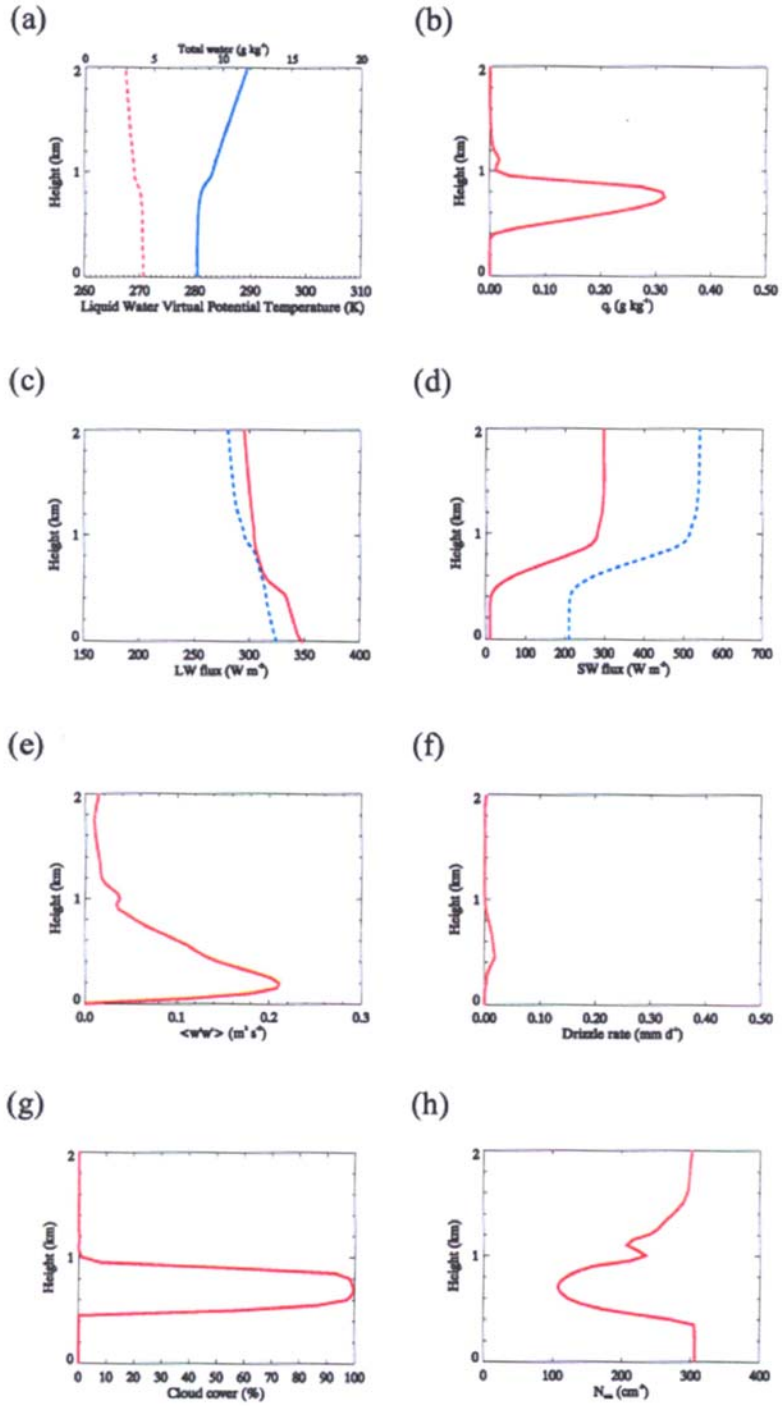

Figure 3. Domain-averaged LES vertical profiles at 4 h for the March 3, 2000, experiment. (a) θ_v (solid) and qt (dashed), (b) liquid water, and (c) LW flux, (d) SW flux. Solid lines are upward fluxes. (e) Vertical velocity variance, (f) drizzle rate, (g) cloud cover, and (h) CCN concentration.

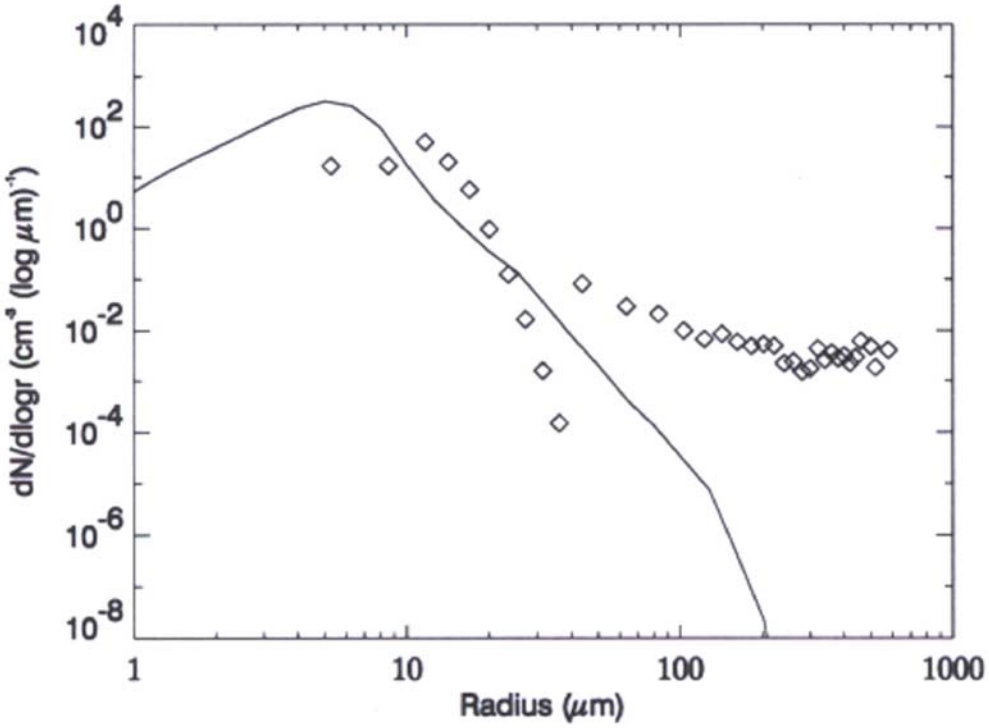

Figure 4. 4 h simulated cloud droplet spectra (solid line) and in situ cloud microphysical data (diamonds) from the FSSP and one-dimensional cloud (1DC) instruments from a height corresponding that of the Citation on flight leg from 1815-1830 UTC.

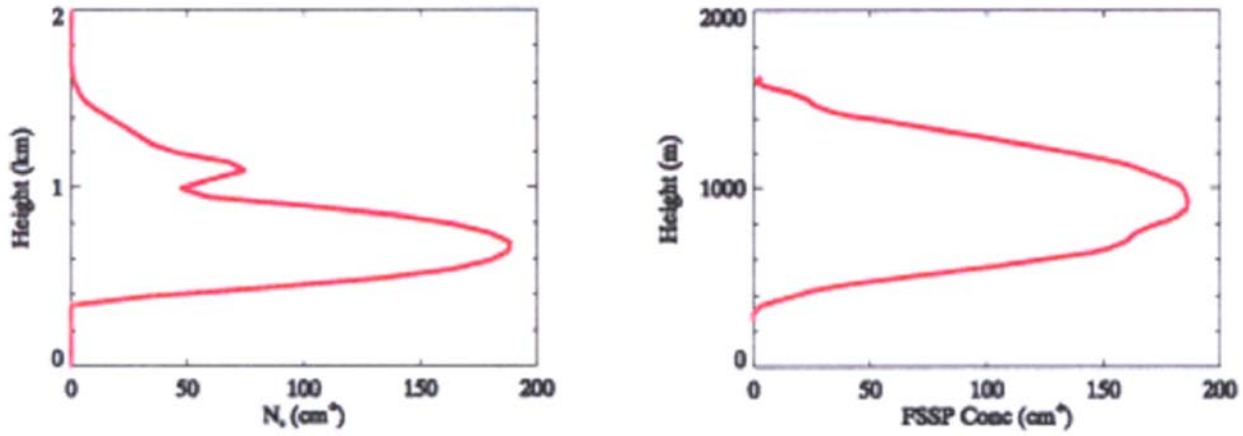

Figure 5. (a) Cloud droplet number concentration at 4 h. (b) FSSP number concentration from a descent leg late in the flight.

at 16 UTC appears to be forced by a region of mesoscale ascent associated with the frontal zone. The high reflectivities after the frontal passage extend to the ground and are probably manifested as strong drizzle.

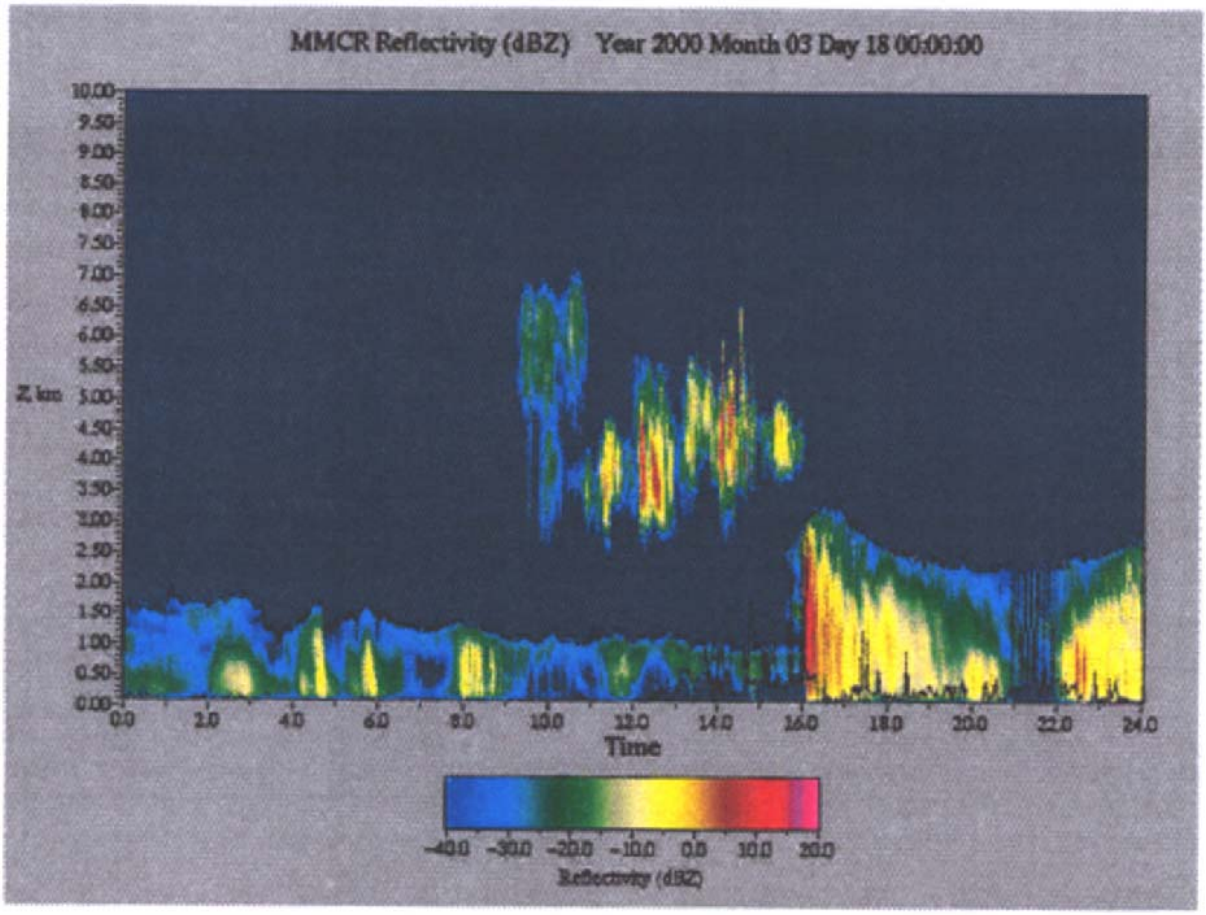

Figure 6. Time-height section of radar reflectivity from the ARM millimeter wave cloud radar (MMCR) for March 18, 2000.

Initial thermodynamic and momentum profiles, both from aircraft data, are shown in Figure 7. In contrast to the March 3 case, the March 18 profiles are quite complicated. A well-missed surface layer, likely driven by surface fluxes and shear, lies underneath a nearly 2 km deep layer of stable stratification. The top of the cloud layer is less stable, overlaid by a jump in temperature and moisture coincident with the top of the cloud. Shear is present over the lowest 600 m of the LES domain, and mean ascent is imposed. Total CCN concentration is assumed to be 85 cm^{-3}, representative of a relatively clean air mass, which in a typical CTBL simulation is conducive to the presence of moderate precipitation (i.e., drizzle). We expect that under strong mesoscale ascent, prodigious precipitation like that seen in the MMCR data will be produced.

The simulation produces a complex cloud structure, maintaining the three layer PBL structure present in the initial profiles (Figure 8a). The surface layer is somewhat more stable than in the initial profile, while the radiatively driven cloud top circulation is more well missed. A rich, multi-layer cloud structure is apparent in the liquid water profile (Figure 8b). The LW radiative flux profile (Figure 8c) shows a greater degree of systematic cloud top cooling compared to the March 3 case, and a more significant SW absorption signal (Figure 8d), a result of the thicker cloud. The vertical velocity variance

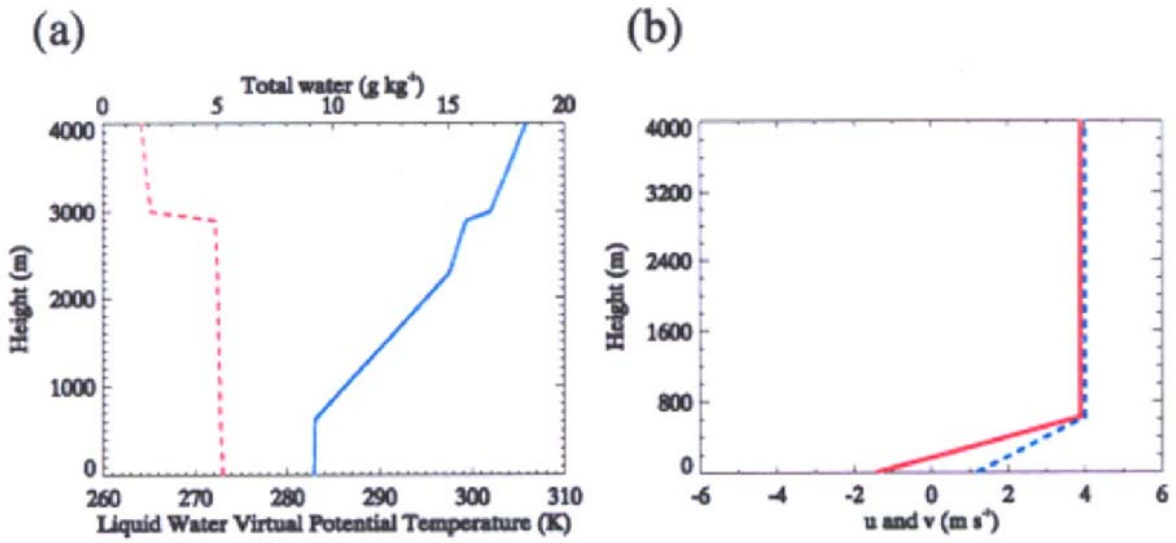

Figure 7. Initial profiles for the March 28, 2000, case. (a) θ_v (solid/blue) and q_t (dashed/red); (b) u (solid/red) and v (dashed/blue).

(Figure 8e) reflects the complexity of the cloud dynamics in three layers: (1) a nearly well missed layer extending from the surface to 800 m, likely driven by surface fluxes and shear, (2) a deep, stably stratified layer, and (3) a well missed layer at cloud top driven by LW cooling.

The precipitation rate (Figure 8f) indicates drizzle production nearly all the way to the surface, where the rate is over 6 mmd^{-1}. The cloud cover and CCN concentration (Figures 8g and 8h) also reflect the complicated, multi-layered cloud structure.

Figure 9 shows a comparison between the LES simulation and Citation cloud droplet data at a height of approximately 1 km. The simulation captures reasonably well the mode of the cloud droplet distribution and the bimodal nature of the distribution. As in the March 3 case, however, our simulations underestimate the number of large droplets. Tuning the initial aerosol profile should produce a closer match to the observed microphysical measurements.

Even thought he simulated and observed cloud droplet spectra are not a perfect match, profiles of the bulk concentration show surprising similarity in shape. The three-layer cloud structure produced by the LES (Figure 10a) seems present, at least to some degree, in the two Citation profiles plotted in Figure 10b. The layered structure appears more pronounced in the simulation, though it is difficult to say whether it is more representative of the mesoscale mean structure. The FSSP data are obtained over only two aircraft profiles (an ascent and descent), so sampling is an issue. In addition, the small domain of the LES (5 km) may not be able to produce the degree of mesocale variability in nature, which if present might tend to smooth some of these features. The quantitative discrepancy between the N_c and FSSP concentrations likely arises from the fact that N_c only considers droplets less than 25 μm in radius, while the FSSP instrument counts droplets of much larger size (up to 60 μm), which are present in this strongly precipitating case.

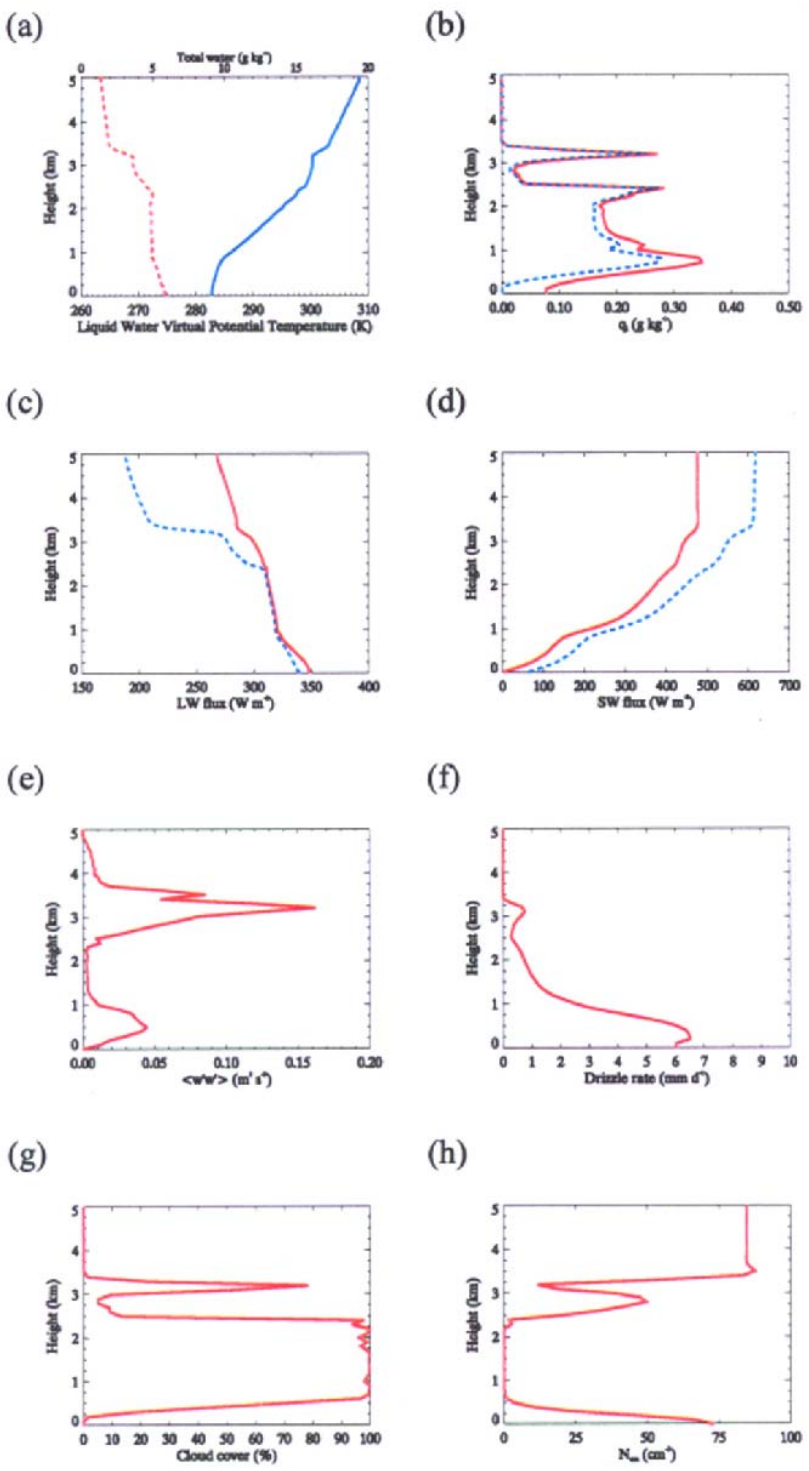

Figure 8. Domain-averaged LES profiles at 4 h for the March 18, 2000, experiment. (a) θ_v (solid) and q_t (dashed), (b) liquid water (solid) and cloud water (dashed). LW (c) and SW (d) radiative flux. Solid lines are upward fluxes. (e) Vertical velocity variance, (f) drizzle rate, (g) cloud cover, and (h) CCN concentration.

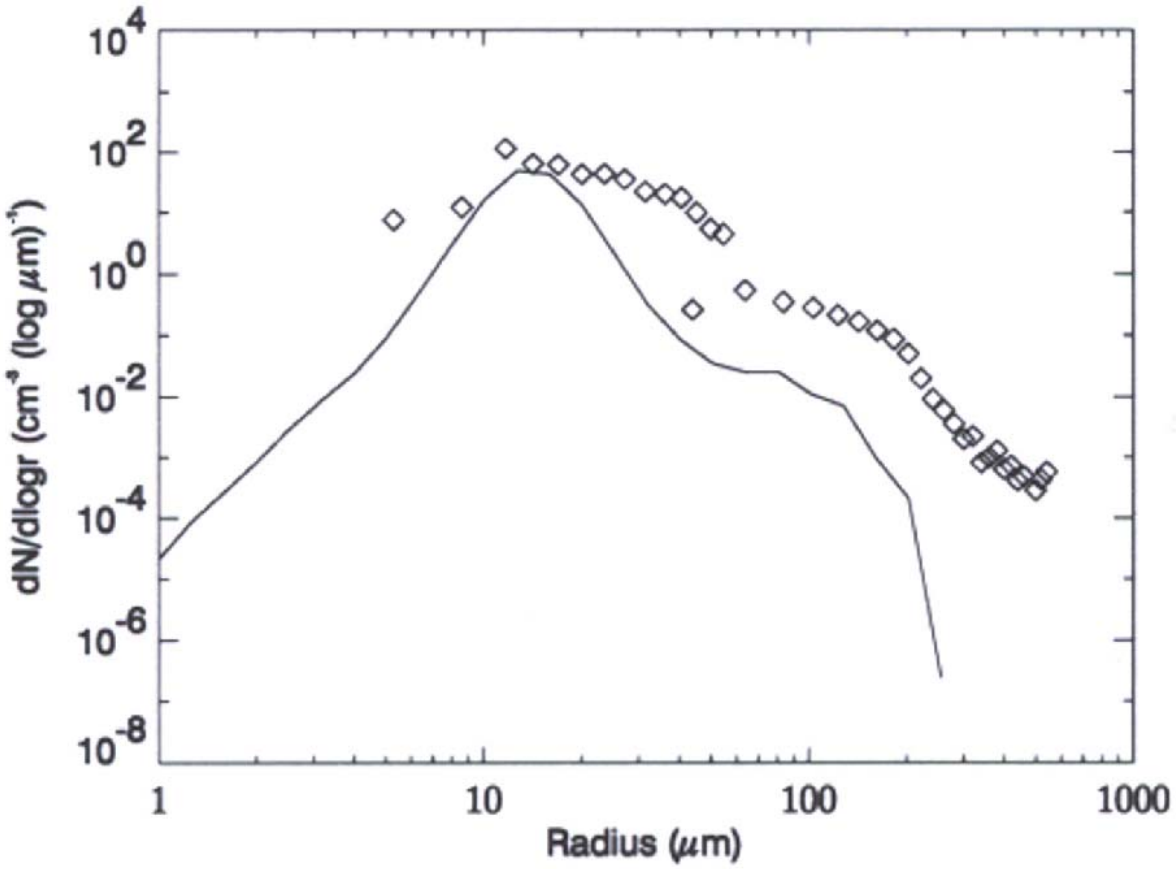

Figure 9. 4 h simulated cloud droplet spectra (solid line) and in situ cloud microphysical data (diamonds) from the FSSP and 1DC instruments from a height corresponding that of the UND Citation on a short flight leg between profiling runs (~1740 UTC).

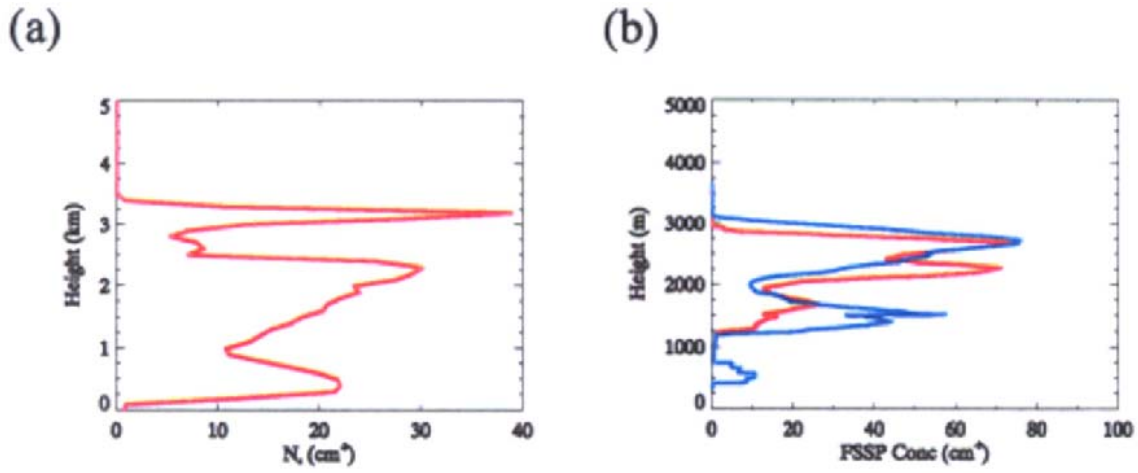

Figure 10. (a) Cloud droplet number concentration at 4 h. (b) FSSP number concentration from sequential ascending (red) and descending (blue) legs late in the flight.

Applicability to Observational Studies of Cloud Variability

In addition to testing the performance of the LES for nontraditional (i.e., general) PBL cases, these simulations and large domain two-dimensional (2D) runs will provide a valuable dataset to study spatial variability of cloud structures. These data will be applied in concert with those from the ARM MMCR to evaluate the amount of the cloud variability that is captured by the MMCR reflectivity. Figure 11 shows scatterplots among two-drop size distribution moments for the two cases. For the strongly drizzling case (March 18), the sixth moment is highly correlated to the fourth (Figure 11c). Since the sixth moment is proportional to radar reflectivity and the fourth to precipitation flux, a strong correlation between the two implies that a characterization of variability in reflectivity (observed by radar) also applies to a subgrid variability in a quantity important to numerical models (precipitation flux). To the

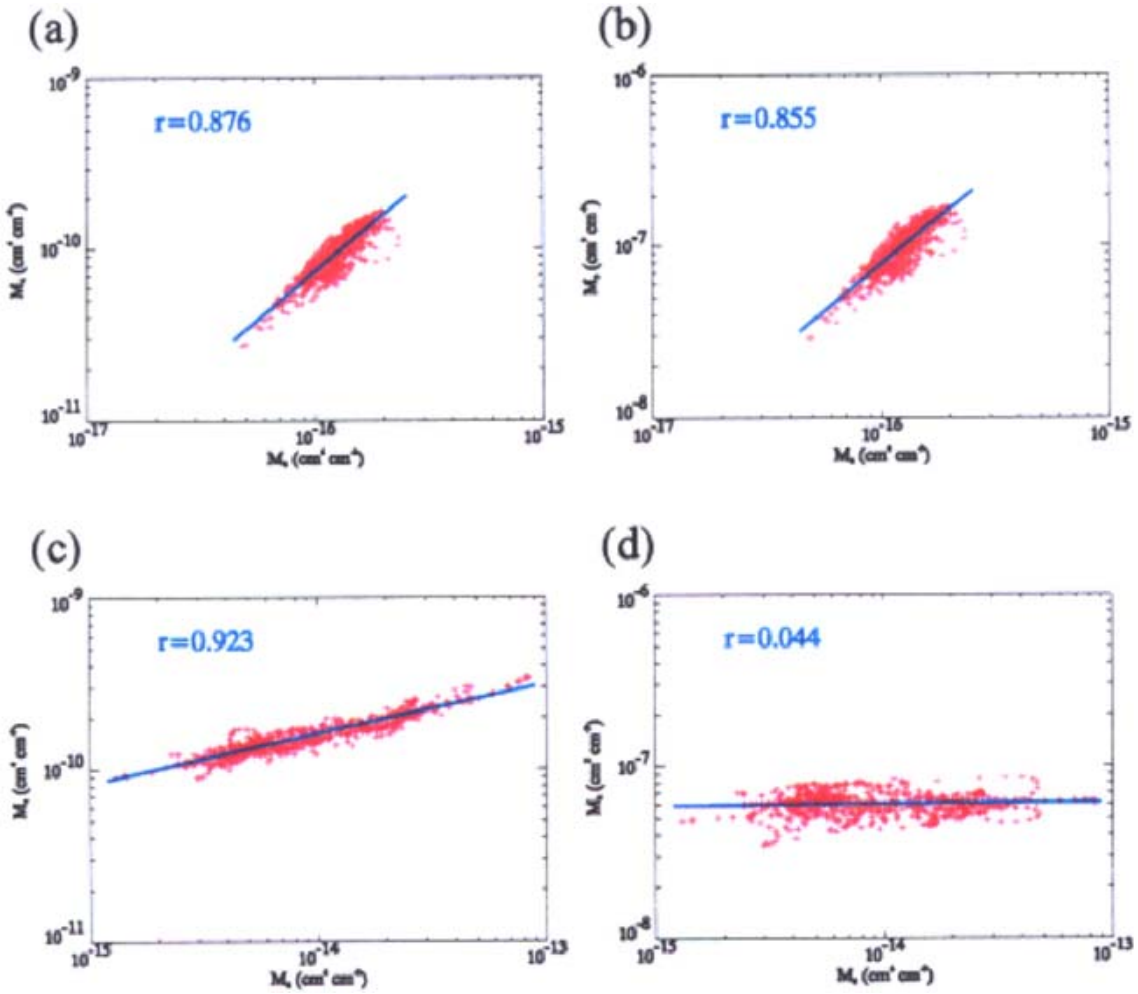

Figure 11. Scatterplots between moments of the simulated drop size distributions for a single vertical model level. Correlation coefficients for each relationship are also shown. (a) March 3 M_6-M_4; (b) March 3 M_6-M_3; (c) March 18 M_6-M_4; and (d) March 18 M_6-M_3.

extent that these correlations are strong, variability between observed quantities (e.g., reflectivity) and model quantities (liquid water, precipitation flux, effective radius) will be related. LES simulations can be used to demonstrate the nature and extent of these relationships.

The March 18 (strongly drizzling; stable) case that exhibits strong correlation between the sixth and fourth moments shows no correlation between sixth and third (proportional to liquid water content). Scatterplots of the March 3 bare quite the opposite, with reasonable correlation between the sixth and third moments. The relationship is the basis for the mathematical "Z-LWC" relationships commonly used to retrieve liquid water content from MMCR reflectivity. Similar correlation is present between the sixth and fourth moments, but the physical significance is somewhat dubious, since the precipitation flux (strongly related to the fourth moment) should be quite small.

Conclusions

We have applied the technique of LES to two nontraditional systems of boundary layer cloud observed during the ARM 2000 Cloud IOP. The first case is a shallow, well-mixed layer topped by a very weak temperature and moisture jump that is not coincident with cloud top. The boundary layer in the second case is deep, filled with cloud, and largely stable, except for a shear- and flux-driven surface layer and a shallow region of radiatively driven missing at cloud top.

When initialized with detailed temperature, water vapor, and liquid water profiles from aircraft data, the LES seems quite capable of producing and maintaining the complex vertical structure present in the observational data. Despite shortcomings with the simulated droplet spectra, behavior of the bulk microphysical quantities such as liquid water content and integrated droplet concentration are quite reasonable. Since the initial aerosol distributions are largely an educated guess to produce the observed cloud drop size distributions, we expect that a tuning of the aerosol spectrum will produce a closer match of the LES droplet spectrum to the aircraft FSSP and 1DC data.

These cases take place in an environment of strong synoptic scale forcing and rapid evolution compared to typical marine CTBLs. Although we neglect the horizontal advection of temperature and moisture, these effects could be easily incorporated into a simulation by simply adding them as source terms in the model equations. We did account for quasi-geostrophic vertical motion through an imposed large-scale ascent/descent (convergence/divergence).

Ultimately, large domain 2D simulations of these and other cases, combined with observations from MMCR, will provide a valuable dataset to study the spatial variability of cloud structures. A better understanding of cloud variability should ultimately lead to an improved understanding and treatment of subgrid heterogeneity in mesoscale, numerical weather prediction, and global climate models.

Acknowledgments

This research was supported by the Environmental Sciences Division of the U.S. Department of Energy (through Battelle PNR Contract 144880-A-Q1 to the Cooperative Institute of Mesoscale Meteorolgical Studies) as part of the Atmospheric Radiation Measurement Program, and by ONR N00014-96-1-0687 and N00014-96-1-1112. Lan Yi provided support with the LES model.

Corresponding Author

David Mechem, dmechem@ou.edu

References

Brown, A. R., et al., 2002: Large-eddy simulation of the diurmal cycle of shallow cumulus convection over land. *Quart. J. Roy. Meteor. Soc*., in press.

Khairoutdinov, M. P., and Y. L. Kogan, 1999: A large-eddy simulation model with explicit microphysics: Validation against aircraft observations of a stratocumulus-topped boundary layer. *J. Atmos. Sci*., **56**, 2115-2131.

Kogan, Y. L., M. P. Khairoutdinov, D. K. Lilly, Z. N. Kogan, and Q. Liu, 1995: Modeling of stratocumulus cloud layers in a large-eddy simulation model with explicit microphysics. *J. Atmos. Sci*., **52**, 2923-2940.

Kosovic, B. and J. A. Curry, 2000: A large-eddy simulation study of a quasi-steady, stably stratified atmospheric boundary layer. *J. Atmos. Sci*., **57**, 1052-1068.

Krueger, S. K., and A. Bergeron, 1994: Modeling the trade cumulus boundary layer. *Atmos Res*., **33**, 169-192.

Moeng, C.-H., 1986: Large-eddy simulation of a stratus-topped boundary layer. Part 1: Structure and budgets. *J. Atmos., Sci*., **43**, 2886-2990.